Signal Processing 115 (2015) 1–8

Contents lists available at ScienceDirect

Signal Processing

journal homepage: www.elsevier.com/locate/sigpro

Fast DOA estimation based on a split subspace decomposition on the array covariance matrix

Feng-Gang Yan [a,*], Yi Shen [b], Ming Jin [a]

[a] Harbin Institute of Technology at Weihai, Weihai 264209, China
[b] Harbin Institute of Technology, Harbin 264209, China

ARTICLE INFO

Article history:
Received 23 June 2014
Received in revised form
19 February 2015
Accepted 10 March 2015
Available online 18 March 2015

Keywords:
Direction-of-arrival (DOA) estimation
Real-valued root multiple signal classification (RV-root-MUSIC)
Split decomposition
Array covariance matrix (ACM)

ABSTRACT

A novel real-valued root multiple signal classification (RV-root-MUSIC) algorithm for estimating the direction-of-arrival (DOA) of multiple narrow-band signals is presented. Compared with the conventional root-MUSIC with a complex subspace decomposition on the entire array covariance matrix (ACM), RV-root-MUSIC exploited a split subspace decomposition on either the real-part of ACM (R-ACM) or the imaginary-part of ACM (I-ACM) with real-valued computations. Unlike the unitary root-MUSIC (U-root-MUSIC) with exploitations on the centro-Hermitian property of ACM, the proposed method developed a new result showing that R-ACM shares the same null subspace with I-ACM, which collides with the intersection of the original noise subspace and its conjugate one. Thanks to the real coefficients, the roots of RV-root-MUSIC appear in conjugate pairs, which allows fast rooting with only real-valued computations. Therefore, both subspace decomposition and polynomial rooting can be implemented with real-valued computations, which hence results in a significant reduction in computational cost as compared to root-MUSIC and U-root-MUSIC. Simulations are conducted to verify the effectiveness of the new technique.

1. Introduction

Estimating the direction-of-arrival (DOA) of multiple narrow-band sources has been intensively addressed since it is an important task that arises in many applications including radar, sonar, wireless communications, speech processing and navigation [1–3]. Over several decades, numerous techniques such as the multiple signal classification (MUSIC) [4] and estimation of signal parameters via rotational invariance techniques (ESPRIT) [5] have been developed. Among those approaches, the MUSIC algorithm firstly exploits the orthogonality between the signal subspace and the noise subspace to achieve a so-called *super-resolution* DOA estimate. Because these two subspaces are perfectly orthogonal to each other when the signal-to-noise ratio (SNR) is sufficiently high, the MUSIC algorithm can resolve two sources as closely-spaced as possible. Another outstanding advantage of the MUSIC algorithm over the other super-resolution methods is that the former can be used with arbitrary array configurations. However, the computational complexity of MUSIC is prohibitively expensive for real-time applications, owing to an involved matrix decomposition step on the array covariance matrix (ACM) for subspace decomposition and a tremendous spectral search step for final DOA estimates [6].

To reduce the complexity, the root-MUSIC algorithm [7] uses the Vandermonde structure of a uniform linear array (ULA) to transform the heavy spectral search step of MUSIC into a simple polynomial rooting one. Although root-MUSIC is only a special case of MUSIC in ULAs, many techniques such as array interpolation (AI) [8], manifold separation technique (MST) [9] and Fourier-domain root

* Corresponding author.
E-mail address: yfglion@163.com (F.-G. Yan).

http://dx.doi.org/10.1016/j.sigpro.2015.03.008
0165-1684/

MUSIC (FD-root-MUSIC) [10] are proposed to extend root-MUSIC to nonuniform arrays (NUAs). Moreover, the former has also been found by theoretical analysis [11] to show an improved performance as compared to the latter. Therefore, root-MUSIC obtains an improved accuracy with a reduced computational load as compared to MUSIC. However, since the subspace decomposition step and the polynomial rooting step in root-MUSIC are based on complex operations, the complexity of root-MUSIC is still high, especially for real-time applications.

Noting that all the computations in the conventional MUSIC are implemented by complex-valued computation, a unitary transformation technique is proposed in [12] to derive a real-valued version of the standard MUSIC (U-MUSIC). Following this idea, a unitary root-MUSIC (U-root-MUSIC) [13] estimator is also proposed to further reduce the complexity of the standard root-MUSIC. It exploits unitary transformation or forward/backward (FB) averaging [14] techniques to transform the array covariance matrix (ACM) into a symmetrical real matrix, then performs subspace decomposition on this real matrix with only real-valued computations. Since one multiplication between two complex variables generally require four times that between two real ones, the complexity of the subspace decomposition step is reduced by U-root-MUSIC as compared to root-MUSIC, approximately by a factor of four [15,16]. Besides, it has been found that U-root-MUSIC also shows improved accuracy as compared to the standard root-MUSIC [17], and thus obtains an increased accuracy with a reduced complexity [18]. However, it is worth noting that the efficient real-valued computations in U-root-MUSIC are only involved in the subspace decomposition stage. In other words, the polynomial rooting stage in U-root-MUSIC still involves complex computations, due to the fact that the polynomial coefficients in U-root-MUSIC are complex.

Therefore, the main purpose of this paper is to reduce the complexity of the standard root-MUSIC with real-valued computations, taking into account both the subspace decomposition- and the polynomial rooting-steps. As a further extension of our previous work in [19], we propose in this paper a novel real-valued root MUSIC (RV-root-MUSIC) algorithm, which finds signal DOAs by polynomial rooting with real-valued computations. Unlike most state-of-the-art unitary approaches including U-root-MUSIC, no unitary transformation and FB-averaging processing is required for the proposed technique since RV-root-MUSIC uses a novel idea of a split subspace decomposition on ACM. By considering the real-part of ACM (R-ACM) and the imaginary-part of ACM (I-ACM) separately, we show that R-ACM shares the same null subspace with I-ACM, which collides with the intersection of the original noise subspace and its conjugate one. As R-ACM and I-ACM are both real matrices, the intersection noise subspace can be estimated by an eigenvalue decomposition (EVD) on R-ACM or by a singular value decomposition (SVD) on I-ACM with real-valued computations. Furthermore, since the polynomial coefficients in RV-root-MUSIC are real, the roots in the proposed approach appear in conjugate pairs of the form $a+jb$, $a-jb$, which allows fast polynomial rooting by using Bairstow's method [20,21] with low-complexity real-valued computations. Therefore, both the subspace decomposition- and the polynomial rooting-steps can be implemented with real-valued computations by RV-root-MUSIC, which gives a further computational efficiency as compared to the popular U-root-MUSIC.

Throughout the paper, vectors and matrices are denoted by lower- and upper-case boldface letters, respectively. In addition, complex- and real-matrix are denoted by single-bar- and double-bar-upper boldface letters, respectively, and $\mathrm{Re}(\cdot)$ and $\mathrm{Im}(\cdot)$ denote the real- and the imaginary-parts of the embraced matrix, respectively.

2. Preliminaries

2.1. Signal models

Consider a ULA composed of M omni-directional sensors with inter-sensor spacing d, where the first one is taken as reference. Supposing there are L uncorrelated narrow-band plane waves with unknown DOAs $\theta_l, l=1,2,\ldots,L$ impinging on the array from far field, the array received data at snapshot $t, t=1,2,\ldots,N$, can be written as

$$\mathbf{x}(t)=\mathbf{A}\mathbf{s}(t)+\mathbf{n}(t). \tag{1}$$

where $\mathbf{s}(t)\in\mathbb{C}^{L\times 1}$ is the signal vector, $\mathbf{n}(t)\in\mathbb{C}^{M\times 1}$ is the additive white Gaussian noises (AWGN) vector, and $\mathbf{A}\in\mathbb{C}^{M\times L}$ is the steering matrix whose column stands for the steering vector, given by [8]

$$\mathbf{a}(\theta)\triangleq\left[1,e^{j\omega_l},e^{j2\omega_l},\ldots,e^{j(M-1)\omega_l}\right]^T \tag{2}$$

where $j\triangleq\sqrt{-1}$, $\omega_l\triangleq(2\pi/\lambda)d\sin\theta_l$ with λ denoting signal average wavelength. The $M\times M$ complex matrix ACM can be written as

$$\begin{aligned}\mathbf{B}&\triangleq E\left\{\mathbf{x}(t)\mathbf{x}^H(t)\right\}\\&=\mathbf{A}\mathbf{B}_s\mathbf{A}^H+\sigma_n^2\mathbf{I}\end{aligned} \tag{3}$$

where $\mathbf{B}_s\triangleq E\left\{\mathbf{s}(t)\mathbf{s}^H(t)\right\}$ is the source covariance matrix and σ_n^2 is the power of AWGN.

For full-rank AWGN, the EVD of matrix $\mathbf{B}$ can be rewritten as

$$\begin{aligned}\mathbf{B}&=\sum_{s=1}^{L}\rho_s\mathbf{e}_s\mathbf{e}_s^H+\sigma_n^2\sum_{t=L+1}^{M}\mathbf{e}_t\mathbf{e}_t^H\\&=\mathbf{E}_s\mathbf{\Lambda}_s\mathbf{E}_s^H+\mathbf{E}_n\mathbf{\Lambda}_n\mathbf{E}_n^H.\end{aligned} \tag{4}$$

where $\mathbf{e}_s\in\mathbb{C}^{M\times 1}, s=1,2,\ldots,L$ are eigenvectors associated with the L most significant eigenvalues ρ_s, $\mathbf{e}_t\in\mathbb{C}^{M\times 1}$, $t=L+1,2,\ldots,M$ are those associated with the $(M-L)$ smallest eigenvalues equaling to σ_n^2, and the range spaces of matrices

$$\begin{aligned}\mathbf{E}_s&\triangleq[\mathbf{e}_1,\mathbf{e}_2,\ldots,\mathbf{e}_L]\\\mathbf{E}_n&\triangleq\left[\mathbf{e}_{L+1},\mathbf{e}_{L+2},\ldots,\mathbf{e}_M\right]\end{aligned} \tag{5}$$

are the so-called signal- and noise-subspace, respectively. In practical situations, the theoretical $\mathbf{B}$ in (3) is unavailable, and ACM is usually estimated by N snapshots of array received datum as follows:

$$\hat{\mathbf{B}} = \frac{1}{N}\sum_{t=1}^{N}\mathbf{x}(t)\mathbf{x}^H(t). \tag{6}$$

Therefore, the EVD of ACM is in fact given by

$$\hat{\mathbf{B}} = \hat{\mathbf{E}}_s\hat{\mathbf{\Lambda}}_s\hat{\mathbf{E}}_s^H + \hat{\mathbf{E}}_n\hat{\mathbf{\Lambda}}_n\hat{\mathbf{E}}_n^H. \tag{7}$$

2.2. MUSIC, root-MUSIC and U-root-MUSIC

According to the orthogonality between span$(\mathbf{E}_s)$ and span$(\mathbf{E}_n)$, the MUSIC algorithm [4] attempts to find the steering vectors which are as orthogonal to the estimated noise subspace as possible in which source DOAs are found by an exhaustive point by point spectral search step as follows:

$$\min_{\theta} f_{\text{MUSIC}}(\theta) = \left\|\hat{\mathbf{E}}_n^H\mathbf{a}(\theta)\right\|^2. \tag{8}$$

Note that this spectral search step is computationally very expensive for real-time applications because for each point, the product $\|\hat{\mathbf{E}}_n^H\mathbf{a}(\theta)\|^2$ must be computed [6,10,19].

For the special geometry of a ULA, the steering vector $\mathbf{a}(\theta)$ in (2) can be rewritten as

$$\mathbf{a}(\theta) = \mathbf{p}(z) \triangleq \left[1, z, z^2, \ldots, z^{M-1}\right]^T \tag{9}$$

where $z \triangleq e^{j\omega_l}$, the root-MUSIC estimator transforms $f_{\text{MUSIC}}(\theta)$ to a polynomial as [7]

$$f_{\text{root-MUSIC}}(z) \triangleq \mathbf{p}^T\left(z^{-1}\right)\hat{\mathbf{E}}_n\hat{\mathbf{E}}_n^H\mathbf{p}(z). \tag{10}$$

Thus, the spectral search step involved in $f_{\text{MUSIC}}(\theta)$ is replaced by finding the L roots of $f_{\text{root-MUSIC}}(z), \hat{z}_l, l = 1, 2, \ldots, L$, which are located closest to the unit circle equivalently, and DOAs are given by

$$\hat{\theta}_l = \arcsin\left(\frac{\lambda}{2\pi d}\angle\hat{z}_l\right), \quad l = 1, 2, \ldots, L. \tag{11}$$

Since $\hat{\mathbf{E}}_n \in \mathbb{C}^{M\times(M-L)}$ is a complex matrix, both the subspace decomposition step and polynomial rooting step in $f_{\text{root-MUSIC}}(z)$ require complex computations accordingly. Therefore, the complexity of root-MUSIC is in fact still high [13].

To further reduce the complexity of root-MUSIC, the U-root-MUSIC [13] algorithm exploits unitary transformation or FB averaging technique [14] to transform ACM into a symmetrical real matrix $\mathbb{B} = \text{Re}\left(\mathbf{U}^H\hat{\mathbf{B}}\mathbf{U}\right)$. Here,

$$\mathbf{U} = \frac{1}{\sqrt{2}}\begin{bmatrix}\mathbf{I} & \text{j}\mathbf{I}\\ \mathbf{J} & -\text{j}\mathbf{J}\end{bmatrix}$$

for M is even, and

$$\mathbf{U} = \frac{1}{\sqrt{2}}\begin{bmatrix}\mathbf{I} & \mathbf{0} & \text{j}\mathbf{I}\\ \mathbf{0}^T & \sqrt{2} & \mathbf{0}^T\\ \mathbf{J} & \mathbf{0} & -\text{j}\mathbf{J}\end{bmatrix}$$

for M is odd, $\mathbf{J}$ is the exchange matrix with ones on its anti-diagonal and zeros elsewhere, $\mathbf{I}$ and $\mathbf{0}$ stand for the identity- and the zero-matrix, respectively. Performing EVD on $\mathbb{B}$ as follows:

$$\mathbb{B} = \mathbb{D}_s\mathbb{U}_s\mathbb{D}_s^T + \mathbb{D}_n\mathbb{U}_n\mathbb{D}_n^T \tag{12}$$

where the subscripts s and n stand for signal- and noise-subspace, respectively. With the real matrix $\mathbb{D}_n$, U-root-MUSIC obtains a polynomial as follows:

$$f_{\text{U-root-MUSIC}}(z) \triangleq \tilde{\mathbf{p}}^T\left(z^{-1}\right)\hat{\mathbb{D}}_n\hat{\mathbb{D}}_n^T\tilde{\mathbf{p}}(z) \tag{13}$$

where $\tilde{\mathbf{p}}(z) \triangleq \mathbf{U}^H\mathbf{p}(z)$. Although matrix $\hat{\mathbb{D}}_n$ is real, it is worth noting that the coefficients in (13) are complex, and consequently, the polynomial rooting step in U-root-MUSIC still requires complex computations.

3. The proposed RV-root-MUSIC algorithm

3.1. Split subspace decomposition on ACM

Let us start our algorithm by considering the intersection of the original noise subspace span$(\mathbf{E}_n)$ and the conjugate one span$(\mathbf{E}_n^*)$, which is given by

$$\text{span}(\mathbb{E}_n) \triangleq \text{span}(\mathbf{E}_n) \cap \text{span}\left(\mathbf{E}_n^*\right). \tag{14}$$

As it is to be shown shortly that $\mathbb{E}_n$ is a real matrix, which can be computed by the EVD of R-ACM or by the SVD of I-ACM with real-valued computations. Clearly, span$(\mathbb{E}_n)$ can be also used to estimate source DOAs since all the vectors in span$(\mathbb{E}_n)$ belong to the noise subspace. Moreover, we have the following important theorem revealing the relationships among span$(\mathbb{E}_n)$ and the null space of R-ACM and that of I-ACM.

Theorem 1. *Using R-ACM to define a new matrix* $\mathbf{Q}$

$$\mathbf{Q} \triangleq \text{Re}(\mathbf{B}) - \sigma_n^2\mathbf{I}. \tag{15}$$

Then we have

$$\text{Null}(\mathbf{Q}) = \text{Null}[\text{Im}(\mathbf{B})] = \text{span}(\mathbb{E}_n). \tag{16}$$

Proof. See Appendix A.

Now, consider the EVD of R-ACM. It follows directly from (16) that $\forall\boldsymbol{\beta} \in \text{span}(\mathbb{E}_n)$, we must have $\boldsymbol{\beta} \in \text{Null}(\mathbf{Q})$, which means that $\mathbf{Q}\boldsymbol{\beta} = \mathbf{0}$, and we further have

$$\text{Re}(\mathbf{B})\boldsymbol{\beta} = \sigma_n^2\boldsymbol{\beta}. \tag{17}$$

Eq. (17) can be identified as the characteristic one for the real-valued matrix Re$(\mathbf{B})$, which means that σ_n^2 is an eigenvalue of Re$(\mathbf{B})$ and $\boldsymbol{\beta}$ is the eigenvector associated with σ_n^2. Since $\boldsymbol{\beta}$ is an arbitrary vector of span$(\mathbb{E}_n)$, $\mathbb{E}_n$ can be computed by the EVD (or SVD) of Re$(\mathbf{B})$ accordingly. Noting that $\mathbf{B} = \mathbf{B}^H$, we have

$$[\text{Re}(\mathbf{B})]^T = \tfrac{1}{2}\left(\mathbf{B} + \mathbf{B}^*\right)^T = \tfrac{1}{2}\left(\mathbf{B}^* + \mathbf{B}\right) = \text{Re}(\mathbf{B}) \tag{18}$$

which implies that Re$(\mathbf{B})$ is a symmetrical real-valued matrix, whose EVD and SVD must require only real-valued computations [22]. Therefore, Im$(\mathbb{E}_n) = \mathbf{0}$, and the EVD (or SVD) of Re$(\mathbf{B})$ can be written as

$$\text{Re}(\mathbf{B}) = \mathbb{E}_s\mathbb{W}_s\mathbb{E}_s^T + \mathbb{E}_n\mathbb{W}_n\mathbb{E}_n^T \tag{19}$$

where subscripts s and n stand for the signal- and the noise-subspaces, respectively.

Next, consider the SVD of Im$(\mathbf{B})$. Noting that $\mathbf{B} = \mathbf{B}^H$, we have

$$\begin{aligned}[\text{Im}(\mathbf{B})]^T &= \frac{1}{2\text{j}}\left(\mathbf{B} - \mathbf{B}^*\right)^T = \frac{1}{2\text{j}}\left(\mathbf{B}^* - \mathbf{B}\right)\\ &= -\text{Im}(\mathbf{B})\end{aligned} \tag{20}$$

which implies that Im(**B**) is an anti-symmetrical real-valued matrix. According to matrix theory [22], the SVD of Im(**B**) must require only real-valued computations (note that the EVD of Im(**B**) may involve complex-valued computations [22]). Therefore, we can write the SVD of Im(**B**) as follows:

$$\mathrm{Im}(\mathbf{B}) = \mathbb{U}_s \mathbb{K}_s \mathbb{V}_s^T + \mathbb{U}_n \mathbb{K}_n \mathbb{V}_n^T. \tag{21}$$

Similarly, subscripts s and n denote the signal- and the noise-subspaces, respectively. Using the facts $\mathbb{K}_n = \mathbf{0}$ [22] as well as $\mathbb{V}_s^T \mathbb{V}_n = \mathbf{0}$ [6] leads to

$$\begin{aligned}\mathrm{Im}(\mathbf{B})\mathbb{V}_n &= \mathbb{U}_s \mathbb{K}_s \mathbb{V}_s^T \mathbb{V}_n + \mathbb{U}_n \mathbb{K}_n \mathbb{V}_n^T \mathbb{V}_n \\ &= \mathbf{0}.\end{aligned} \tag{22}$$

Thus, the columns of $\mathbb{V}_n$ offer an orthogonal basis for Null[Im(**B**)]. According to (16), $\mathbb{V}_n$ can be further taken as an orthogonal basis of span($\mathbb{E}_n$). Thus, span($\mathbb{V}_n$) = span($\mathbb{E}_n$), and the SVD of Im(**B**) can be rewritten as

$$\mathrm{Im}(\mathbf{B}) = \mathbb{U}_s \mathbb{K}_s \mathbb{V}_s^T + \mathbb{U}_n \mathbb{K}_n \mathbb{E}_n^T. \tag{23}$$

From (19) and (23), we see clearly that $\mathbb{E}_n$ can be computed by a split subspace decomposition on R-ACM or I-ACM with real-valued computations.

3.2. The proposed method

With $\mathbb{E}_n$ computed by the split subspace decompositions on R-ACM or I-ACM, we can use the real matrix $\mathbb{E}_n$ to obtain a polynomial with real-valued coefficients as follows:

$$f_{\mathrm{RV-root-MUSIC}}(z) \triangleq \mathbf{p}^T(z^{-1})\widehat{\mathbb{E}}_n \widehat{\mathbb{E}}_n^T \mathbf{p}(z). \tag{24}$$

It is worth noting that all the coefficients in $f_{\mathrm{RV-root-MUSIC}}(z)$ are real, which is different from those in $f_{\mathrm{root-MUSIC}}(z)$ and $f_{\mathrm{U-root-MUSIC}}(z)$. $f_{\mathrm{RV-root-MUSIC}}(z)$ has an important property, given by the following theorem.

Theorem 2. *The roots of $f_{\mathrm{RV-root-MUSIC}}(z)$ appear in both conjugate- and conjugate reciprocal-pairs, that is, if z_0 is a root of $f_{\mathrm{RV-root-MUSIC}}(z)$, both z_0^* and $\tilde{z}_0 \triangleq 1/z_0^*$ are two roots of $f_{\mathrm{RV-root-MUSIC}}(z)$ as well.*

Proof. See Appendix B.

Theorem 2 indicates that the roots of $f_{\mathrm{RV-root-MUSIC}}(z)$ are different from those of $f_{\mathrm{root-MUSIC}}(z)$, which is shown in Figs. 1 and 2 for more clear illustrations. In the figures, two sources at $\theta_1 = 20^\circ$ and $\theta_2 = 40^\circ$ are considered, where the simulation parameters are set as M=9, SNR = 5 dB and N=200. As it is seen from Fig. 1 that the roots of $f_{\mathrm{root-MUSIC}}(z)$ appear in only conjugate reciprocity pairs [7]. However, it is concluded from Fig. 2 that the roots of $f_{\mathrm{RV-root-MUSIC}}(z)$ appear in both conjugate- and conjugate reciprocal-pairs. These differences can be also observed by comparing the proposed method with the U-root-MUSIC algorithm.

As the roots of $f_{\mathrm{RV-root-MUSIC}}(z)$ appear in conjugate pairs with the form $a+jb, a-jb$, Bairstow's method [20,21] can be applied to find the roots of $f_{\mathrm{RV-root-MUSIC}}(z)$ with low-complexity real-valued computations. Therefore, the polynomial rooting step in RV-root-MUSIC can be also implemented with fast real-valued computations, which leads to further computational efficiency as compared to the U-root-MUSIC technique.

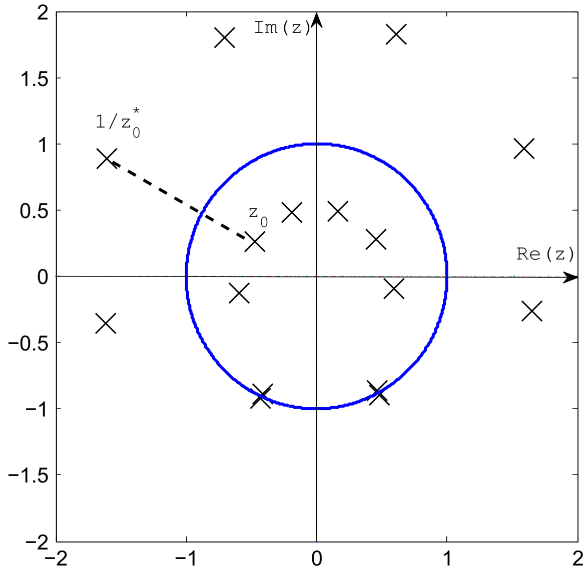

Fig. 1. Roots of root-MUSIC.

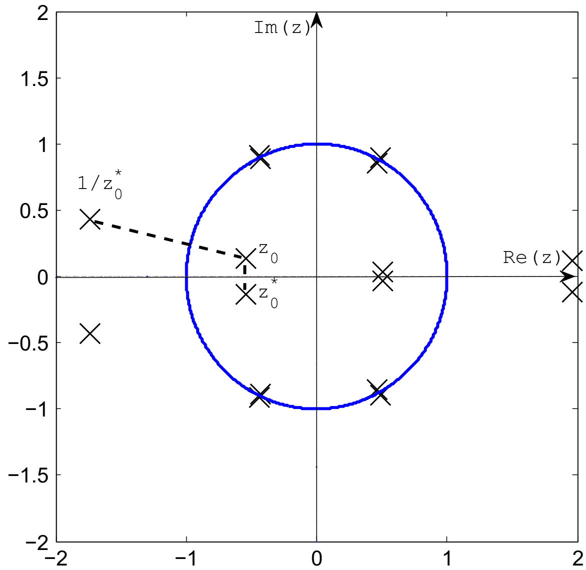

Fig. 2. Roots of RV-root-MUSIC.

With the above analysis, supposing z_l is a root of $f_{\mathrm{RV-root-MUSIC}}(z)$ that lies closest to the unit circle, then z_l or z_l^* must be two roots corresponding to signal DOAs. To resolve the problem of estimation ambiguity with low-complexity, the conventional beamforming [25] can be used to select the right root between z_l or z_l^* for the true DOA. Detailed steps for implementing the proposed RV-root-MUSIC algorithm are summarized in Table 1.

We end up this subsection by a comparison of complexity between conventional root-MUSIC, U-root-MUSIC and the proposed method. The computation of the coefficients of $f_{\mathrm{RV-root-MUSIC}}(z)$ is implemented via a real-valued eigen-decomposition on R-ACM or I-ACM while that of $f_{\mathrm{root-MUSIC}}(z)$ is implemented by a complex one on the

Table 1
The proposed RV-root-MUSIC algorithm.

- **Step 1**: Receive N snapshots of the array output $\widehat{\mathbf{x}}(t)_{t=1}^{N}$;
- **Step 2**: Estimate $\widehat{\mathbf{B}}$ by (6) and obtain Re $(\widehat{\mathbf{B}})$ and Im $(\widehat{\mathbf{B}})$.
- **Step 3**: Compute the EVD/SVD of Re $(\widehat{\mathbf{B}})$ by (18) (or the SVD of Im $(\widehat{\mathbf{B}})$ by (22) to get $\mathbb{E}_n$;
- **Step 4**: Construct $f_{\text{RV-root-MUSIC}}\ (z)$ by (23), and find its L pairs of roots $\widehat{z}_l, \widehat{z}_l^*, l=1,2,\ldots,L$, which lie closest to the unit circle;
- **Step 5**: Calculate the L pairs of possible signal DOAs $\widehat{\theta}_l, -\widehat{\theta}_l, l=1,2,\ldots,L$ by (11);
- **Step 6**: Select the L true DOAs among $\widehat{\theta}_l, -\widehat{\theta}_l, l=1,2,\ldots,L$ by maximizing the product $\|\mathbf{a}^H(\theta)\widehat{\mathbf{B}}\mathbf{a}(\theta)\|^2$.

entire ACM. Thus, the complexity of subspace decomposition involved in the proposed method is approximately four times lower than that in the standard root-MUSIC. This computational efficiency is comparable to that of U-root-MUSIC since U-root-MUSIC also exploited a real-valued eigen-decomposition. However, since the roots of $f_{\text{RV-root-MUSIC}}(z)$ can be also found by real-valued computations while those of $f_{\text{root-MUSIC}}(z)$ and $f_{\text{U-root-MUSIC}}(z)$ cannot, the overall computational cost of RV-root-MUSIC is much lower than those of conventional root-MUSIC and U-root-MUSIC.

4. Simulation results

Computer simulations with numerical scenarios are conducted to assess the proposed method. Throughout the simulations, 1000 independent Monte Carlos have been used on a ULA with half wavelength apart. For the root mean square error (RMSE) comparison, the unconditional Cramer–Rao low (CRLB) given in [26] is also applied for reference, where the RMSE for the estimates of source incident angle θ is defined as

$$\text{RMSE} \triangleq \sqrt{\frac{1}{1000}\sum_{i=1}^{1000}\left(\widehat{\theta}_i-\theta\right)^2} \tag{25}$$

where θ is the true DOA and $\widehat{\theta}_i$ represents the estimated value of the DOA of the i-th trial.

The first simulation compares the RMSE for DOA estimation by different algorithms, including MUSIC [4], ESPRIT [5], root-MUSIC [7], U-root-MUSIC [13] and the proposed method. In this simulation, $L=2$ sources at $\theta_1=20^\circ$ and $\theta_2=40^\circ$ are considered, where the number of sensors is set as $M=9$. For the search-based algorithm MUSIC, a coarse gird 1° is firstly used to get candidate peaks, and a fine one 0.0051° is secondly applied around the candidate peaks for final DOA estimates.

Fig. 3 demonstrates the RMSEs against the SNR, where the number of snapshots is set as $N=200$ and the SNR varies over a wide range from SNR $=-10$ dB to SNR $=10$ dB. It can be concluded from Fig. 3 that convectional MUSIC, root-MUSIC and U-root-MUSIC slightly outperform our method at low SNRs (SNR <0 dB). However, at high SNRs (SNR >0 dB), the proposed method shows a very close performance to the above three algorithms. It is also concluded from Fig. 3 that the proposed method has a much better performance than ESPRIT.

To further compare the performances of the above four algorithms, Fig. 4 plots RMSEs of different algorithms as functions of the number of snapshots, where the SNR is

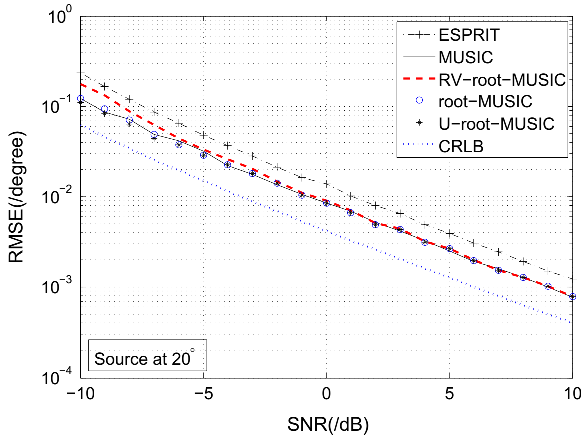

Fig. 3. RMSE against the SNRs.

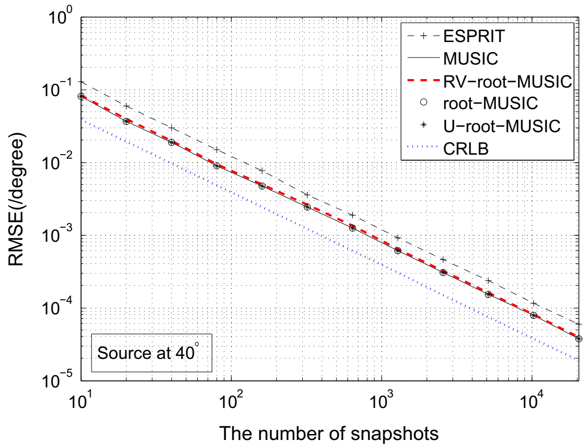

Fig. 4. RMSE against the number of snapshots.

fixed as SNR $=5$ dB and the number of snapshots varies over a wide range from $N=5\times2^1$ to $N=5\times2^{12}$. It can be seen clearly from Fig. 4 that RV-root-MUSIC shows a similar performance to MUSIC, root-MUSIC and U-root-MUSIC over the wide range of $N=5\times2^1$ to $N=5\times2^{12}$. Moreover, it is seen again that the proposed method indeed shows a much higher accuracy than ESPRIT.

To see more clearly the performance of the proposed method, we examine the performance of different algorithms in a special scenario in Fig. 5, where $L=2$ closely-spaced sources at $\theta_1=20^\circ$ and $\theta_2=20^\circ+\Delta\theta$ are considered with $M=9$ sensors, where $\Delta\theta$ varies from $\Delta\theta=2^\circ$ to $\Delta\theta=15^\circ$.

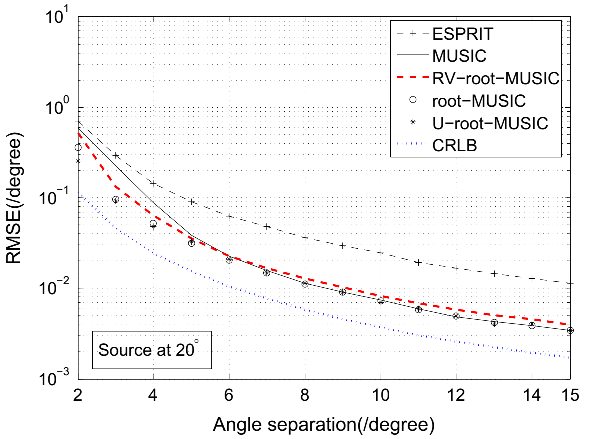

Fig. 5. RMSE against angle separation.

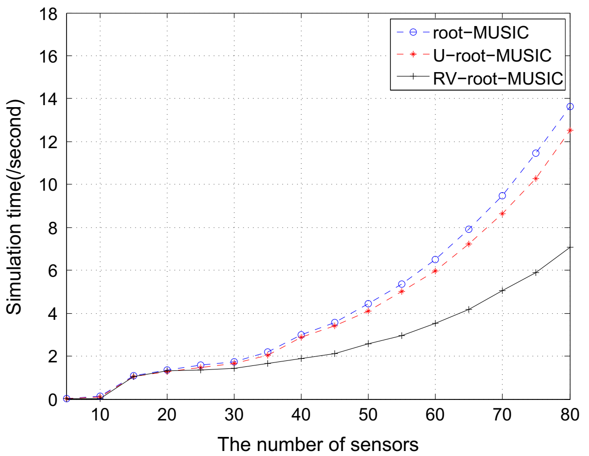

Fig. 6. Simulation time against the number of sensors.

Throughout this simulation, the SNR and the numbers of snapshots are fixed as SNR = 5 dB and N=200, respectively.

It can be seen from Fig. 5 that the proposed method slightly outperforms the conventional MUSIC algorithm when $\Delta\theta < 6^\circ$ while the standard root-MUSIC and U-root-MUSIC slightly outperform our method on the other hand. For $\Delta\theta > 6^\circ$, MUSIC, root-MUSIC, U-root-MUSIC and the proposed technique show a similar performance, which is much better than ESPRIT.

The last simulation verifies the efficiency of the proposed approach as well as verifies the computational complexity analysis by comparing the simulation times of DOA estimates by root-MUSIC, U-root-MUSIC and RV-root-MUSIC as functions of the number of sensors in Fig. 6. The simulated results are given by a PC with Intel(R) Core(TM) Duo T5870 2.0 GHz CPU and 1 GB RAM by running the Matlab codes in the same environment.

It can be seen from Fig. 6 that RV-root-MUSIC is the most efficient one among the three estimators. More specifically, for small numbers of sensors ($M \le 20$), the three algorithms cost a similar time. However, for large numbers of sensors ($M > 20$), RV-root-MUSIC shows an obvious efficiency advantage over the other two techniques. This may be caused by the heavy computational load of the polynomial rooting step when the number of sensors is large.

5. Conclusions

We have proposed a novel computationally efficient RV-root-MUSIC algorithm for DOA estimation, which exploits the idea of a split subspace decomposition on the real-part and the imaginary-part of the ACM while most state-of-the-art DOA estimators are based on the entire ACM. This is resulted from the newly developed result that the real-part or the imaginary-part of ACM shares the same null subspace, which equals to the intersection of the original noise subspace and its conjugate one. Compared with U-root-MUSIC with only a real-valued subspace decomposition, both tasks of subspace decomposition and polynomial rooting can be implemented by real-valued computations in RV-root-MUSIC. Simulations illustrate that the proposed approach has a similar performance to the conventional MUSIC and root-MUSIC approaches while its complexity is about four times lower than root-MUSIC.

Acknowledgements

This work is supported by Shandong Provincial Natural Science Foundation (No. ZR2014FQ003), China.

Appendix A. Proof of Theorem 1

Noting that span($\mathbb{E}_n$) is a subset of span($\mathbf{E}_n$) as well as that of span($\mathbf{E}_n^*$), we must have span($\mathbb{E}_n$) $\subseteq$ span($\mathbf{E}_n^*$) and span($\mathbb{E}_n$) $\subseteq$ span($\mathbf{E}_n$). Therefore, we further have span($\mathbb{E}_n$) $\perp$ span($\mathbf{A}$) and span($\mathbb{E}_n$) $\perp$ span($\mathbf{A}^*$). Post-multiplying the left- and the right-sides of (3) by $\mathbb{E}_n$, we obtain

$$\mathbf{B}\mathbb{E}_n = \mathbf{A}\mathbf{B}_s\mathbf{A}^H\mathbb{E}_n + \sigma_n^2\mathbb{E}_n = \sigma_n^2\mathbb{E}_n. \tag{A.1}$$

Similarly, post-multiplying the left- and the right-sides of the conjugate version of (3) by $\mathbb{E}_n$ leads to

$$\mathbf{B}^*\mathbb{E}_n = \mathbf{A}^*\mathbf{B}_s^*\mathbf{A}^T\mathbb{E}_n + \sigma_n^2\mathbb{E}_n = \sigma_n^2\mathbb{E}_n. \tag{A.2}$$

Adding (A.1) and (A.2) as well as using (15), we have

$$[\mathrm{Re}(\mathbf{B}) - \sigma_n^2\mathbf{I}]\mathbb{E}_n = \mathbf{Q}\mathbb{E}_n = \mathbf{0}. \tag{A.3}$$

According to matrix theory [22], the columns of $\mathbb{E}_n$ must belong to the null subspace of $\mathbf{Q}$. Thus, span($\mathbb{E}_n$) is a subset of the null subspace of $\mathbf{Q}$ accordingly, and we have

$$\mathrm{span}(\mathbb{E}_n) \subseteq \mathrm{Null}(\mathbf{Q}). \tag{A.4}$$

On the other hand, let us assume that $\boldsymbol{\beta}$ is a vector of Null($\mathbf{Q}$), which means that $\mathbf{Q}\boldsymbol{\beta} = \mathbf{0}$. Using (3) and (15), matrix $\mathbf{Q}$ can be rewritten as

$$\begin{aligned}\mathbf{Q} &= \tfrac{1}{2}(\mathbf{B}+\mathbf{B}^*) - \sigma_n^2\mathbf{I}\\ &= \tfrac{1}{2}\left(\mathbf{A}\mathbf{B}_s\mathbf{A}^H + \sigma_n^2\mathbf{I} + \mathbf{A}^*\mathbf{B}_s^*\mathbf{A}^T + \sigma_n^2\mathbf{I}\right) - \sigma_n^2\mathbf{I}\\ &= \tfrac{1}{2}\left(\mathbf{A}\mathbf{B}_s\mathbf{A}^H + \mathbf{A}^*\mathbf{B}_s^*\mathbf{A}^T\right).\end{aligned} \tag{A.5}$$

Therefore, we have

$$\mathbf{A}\mathbf{B}_s\mathbf{A}^H\boldsymbol{\beta} + \mathbf{A}^*\mathbf{B}_s^*\mathbf{A}^T\boldsymbol{\beta} \triangleq \mathbf{A}\boldsymbol{\xi} + \mathbf{A}^*\boldsymbol{\zeta} = \mathbf{0} \tag{A.6}$$

where

$$\begin{cases} \boldsymbol{\xi} \triangleq \mathbf{B}_s\mathbf{A}^H\boldsymbol{\beta} \\ \boldsymbol{\zeta} \triangleq \mathbf{B}_s^*\mathbf{A}^T\boldsymbol{\beta}. \end{cases} \tag{A.7}$$

Expanding $\mathbf{A}\boldsymbol{\xi}$ and $\mathbf{A}^*\boldsymbol{\zeta}$ as weighted sums of the columns of $\mathbf{A}$ and $\mathbf{A}^*$, respectively, (A.6) can be rewritten as

$$\sum_{i=1}^{L}\left[\xi_i\mathbf{a}(\theta_i)+\zeta_i\mathbf{a}(-\theta_i)\right]=\mathbf{0}, \quad \theta_i \in \left[-\frac{\pi}{2},\frac{\pi}{2}\right] \tag{A.8}$$

where the fact $\mathbf{A}^*=\mathbf{A}(-\boldsymbol{\theta})$ is used, and ξ_i and ζ_i are the i-th element of $\boldsymbol{\xi}$ and $\boldsymbol{\zeta}$, respectively. According to array ambiguity restriction [23,24], (A.8) holds if and only if $\xi_i=\zeta_i=0, i=1,2,\ldots,L$, which means that

$$\boldsymbol{\xi}=\boldsymbol{\zeta}=\mathbf{0}. \tag{A.9}$$

Because $\mathbf{B}_s$ is invertible, it follows from (A.9) that $\mathbf{A}^H\boldsymbol{\beta}=\mathbf{A}^T\boldsymbol{\beta}=\mathbf{0}$, and hence $\boldsymbol{\beta}\in\text{span}(\mathbf{E}_n)$, $\boldsymbol{\beta}\in\text{span}(\mathbf{E}_n^*)$. This implies that $\boldsymbol{\beta}\in\text{span}(\mathbb{E}_n)$, and we further have

$$\text{Null}(\mathbf{Q})\subseteq\text{span}(\mathbb{E}_n). \tag{A.10}$$

Combining (A.4) and (A.10), we finally have

$$\text{Null}(\mathbf{Q})=\text{span}(\mathbb{E}_n). \tag{A.11}$$

On the other hand, subtracting (A.2) from (A.1) yields $(\mathbf{B}-\mathbf{B}^*)\mathbb{E}_n=2\text{j}\text{Im}(\mathbf{B})\mathbb{E}_n=\mathbf{0}$, which implies that $\text{span}(\mathbb{E}_n)\subseteq\text{Null}[\text{Im}(\mathbf{B})]$. Oppositely, assume that $\boldsymbol{\gamma}\in\text{Null}[\text{Im}(\mathbf{B})]$, then we have $\text{Im}(\mathbf{B})\boldsymbol{\gamma}=\mathbf{0}$, which is equivalent to $(\mathbf{B}-\mathbf{B}^*)\boldsymbol{\gamma}=\mathbf{0}$. Therefore, we further have $\mathbf{A}\mathbf{B}_s\mathbf{A}^H\boldsymbol{\gamma}-\mathbf{A}^*\mathbf{B}_s^*\mathbf{A}^T\boldsymbol{\gamma}\triangleq\mathbf{A}\boldsymbol{\omega}-\mathbf{A}^*\boldsymbol{\nu}=\mathbf{0}$, where $\boldsymbol{\omega}\triangleq\mathbf{B}_s\mathbf{A}^H\boldsymbol{\gamma}$ and $\boldsymbol{\nu}\triangleq\mathbf{B}_s^*\mathbf{A}^T\boldsymbol{\gamma}$. Using the array ambiguity restriction [20], we can similarly prove that $\text{Null}[\text{Im}(\mathbf{B})]\subseteq\text{span}(\mathbb{E}_n)$. The above analysis shows that

$$\text{Null}[\text{Im}(\mathbf{B})]=\text{span}(\mathbb{E}_n). \tag{A.12}$$

which completes the proof. □

Appendix B. Proof of Theorem 2

Rewrite $f_{\text{RV-root-MUSIC}}(z)$ as

$$f_{\text{RV-root-MUSIC}}(z)=\sum_{k=-(M-1)}^{M-1}C_kz^k \tag{B.1}$$

where $C_k, k=-(M-1),\ldots,-1,0,1,\ldots,M-1$ are the coefficients of z^k in $\mathbf{p}^T(z^{-1})\widehat{\mathbb{E}}_n\widehat{\mathbb{E}}_n^T\mathbf{p}(z)$. Let $\left(\widehat{\mathbb{E}}_n\widehat{\mathbb{E}}_n^T\right)_{s,t}$ be the s-th row and t-th column element of $\widehat{\mathbb{E}}_n\widehat{\mathbb{E}}_n^T$, then we have

$$\begin{aligned}\sum_{k=-(M-1)}^{M-1}C_kz^k &= \mathbf{p}^T(z^{-1})\widehat{\mathbb{E}}_n\widehat{\mathbb{E}}_n^T\mathbf{p}(z)\\ &=\sum_{s=1}^{M-1}\sum_{t=1}^{M-1}z^{-(s-1)}\left(\widehat{\mathbb{E}}_n\widehat{\mathbb{E}}_n^T\right)_{s,t}z^{t-1}\\ &=\sum_{s=1}^{M-1}\sum_{t=1}^{M-1}\left(\widehat{\mathbb{E}}_n\widehat{\mathbb{E}}_n^T\right)_{s,t}z^{t-s}\end{aligned} \tag{B.2}$$

which implies that

$$\begin{aligned}C_k&=\sum_{s=1}^{M-1}\left(\widehat{\mathbb{E}}_n\widehat{\mathbb{E}}_n^T\right)_{s,s+k}\\ &=\sum_{s=1}^{M-1}\left(\widehat{\mathbb{E}}_n\widehat{\mathbb{E}}_n^T\right)_{s+k,s}\\ &=C_{-k}.\end{aligned} \tag{B.3}$$

Assume that z_0 is a root of $f_{\text{RV-root-MUSIC}}(z)$ and taking into account $C_k\in\mathbb{R}, k=-(M-1),\ldots,-1,0,1,\ldots,M-1$, we obtain

$$\begin{aligned}0&=\sum_{k=-(M-1)}^{M-1}C_kz_0^k\\ &=\left(\sum_{k=-(M-1)}^{M-1}C_kz_0^k\right)^*\\ &=\sum_{k=-(M-1)}^{M-1}C_k(z_0^*)^k.\end{aligned} \tag{B.4}$$

Therefore, z_0^* is a root of $f_{\text{RV-root-MUSIC}}(z)$. Besides, it follows directly from (B.3) and (B.4) that

$$\begin{aligned}0&=\sum_{k=-(M-1)}^{M-1}C_k(z_0^*)^k\\ &=\sum_{k=-(M-1)}^{M-1}C_{-k}(\tilde{z}_0)^{-k}\\ &=\sum_{k=-(M-1)}^{M-1}C_k(\tilde{z}_0)^k.\end{aligned} \tag{B.5}$$

Eq. (B.5) shows that $\tilde{z}_0=1/z_0^*$ is also a root of $f_{\text{RV-root-MUSIC}}(z)$. □

References

[1] J. Krim, M. Viberg, Two decades of array signal processing research: the parametric approach, IEEE Signal Process. Mag. 13 (July (3)) (1996) 67–94.

[2] A. Khabbazibasmenj, A. Hassanien, S.A. Voroyov, M.W. Morency, Efficient transmit beamspace design for search-free based DOA estimation in MIMO radar, IEEE Trans. Signal Process. 62 (June (6)) (2014) 1490–1500.

[3] Pec Rothna, Hong Tae Howan, Cho Yong Soo, Searching and DoA estimation for a mobile relay station in a multipath environment, J. Commun. Netw. 15 (April (2)) (2013) 191–197.

[4] R.O. Schmidt, Multiple emitter location and signal parameter estimation, IEEE Trans. Antennas Propag. 34 (March (3)) (1986) 276–280.

[5] R. Roy, T. Kailath, ESPRIT-estimation of signal parameters via rotational invariance techniques, IEEE Trans. Signal Process. 37 (July (7)) (1989) 984–995.

[6] F.G. Yan, M. Jin, X.L. Qiao, Low-complexity DOA estimation based on compressed MUSIC and its performance analysis, IEEE Trans. Signal Process. 61 (April (8)) (2013) 1915–1930.

[7] A. Barabell, Improving the resolution performance of eigenstructure-based direction-finding algorithms, in: Proceedings of ICASSP'83, April 1983, pp. 336–339.

[8] P. Hyberg, M. Jansson, B. Ottersten, Array interpolation and DOA MSE reduction, IEEE Trans. Signal Process. 53 (December (12)) (2005) 4464–4471.

[9] F. Belloni, A. Richter, V. Koivunen, DoA estimation Via manifold separation for arbitrary array structures, IEEE Trans. Signal Process. 55 (October (10)) (2007) 4800–4810.

[10] Michael Rübsamen, Alex B. Gershman, Direction-of-arrival estimation for nonuniform sensor arrays: from manifold separation to fourier domain MUSIC methods, IEEE Trans. Signal Process. 57 (February) (2009) 588–599.

[11] B.D. Rao, K.V.S. Hari, Performance analysis of root-MUSIC, IEEE Trans. Acoust. Speech Signal Process. 37 (December (12)) (1989) 1939–1949.

[12] K.C. Huarng, C.C. Yeh, A unitary transformation method for angle-of-arrival estimation, IEEE Trans. Signal Process. 39 (April) (1991) 975–977.

[13] M. Pesavento, A.B. Gershman, M. Haardt, Unitary root-MUSIC with a real-valued eigendecomposition: a theoretical and experimental performance study, IEEE Trans. Signal Process. 48 (May (5)) (2000) 1306–1314.

[14] D.A. Linebarger, R.D. DeGroat, E.M. Dowling, Efficient direction-finding methods employing forward-backward averaging, IEEE Trans. Signal Process. 42 (August (8)) (1994) 2136–2145.
[15] A.B. Gershman, P. Stoica, On unitary and forward–backward MODE, Dig. Signal Process. 9 (February (2)) (1999) 67–75.
[16] N. Yilmazer, J. Koh, T.K. Sarkar, Utilization of a unitary transform for efficient computation in the matrix pencil method to find the direction of arrival, IEEE Trans. Signal Process. 54 (January) (2006) 175–181.
[17] C. Qian, L. Huang, H.C. So, Improved unitary root-MUSIC for DOA estimation based on pseudo-noise resampling, IEEE Signal Process. Lett. 21 (May (2)) (2014) 140–144.
[18] M. Haardt, J.A. Nossek, Unitary ESPRIT: how to obtain increased estimation accuracy with a reduced computational burden, IEEE Trans. Signal Process. 43 (May (5)) (1995) 1232–1242.
[19] F.G. Yan, M. Jin, S. Liu, X.L. Qiao, Real-valued MUSIC for efficient direction estimation with arbitrary array geometries, IEEE Trans. Signal Process. 62 (March (6)) (2014) 1548–1560.
[20] J. Selva, Computation of spectral and root MUSIC through real polynomial rooting, IEEE Trans. Signal Process. 53 (May (5)) (2005) 1923–1927.
[21] W.H. Press, et al., Numerical recipes in C, Cambridge University Press, Cambridge, UK, 1997.
[22] Gene H. Golub, Chares H. Van Loan, Matirx Computations, The Johns Hopkins University Press, Baltimore, MD, 1996.
[23] C. Proukakis, A. Manikas, Study of ambiguities of linear arrays, in: Proceedings of ICASSP, vol. 4, April 1994, pp. 549–552.
[24] K.C. Tan, Z. Goh, A detailed derivation of arrays free of higher rank ambiguities, IEEE Trans. Signal Process. 44 (February (2)) (1996) 351–359.
[25] V. Vasylyshyn, Improving the performance of Root-MUSIC via pseudo-noise resampling and conventional beamformer, in: 2011 Conference on Microwaves, Radar and Remote Sensing Symposium (MRRS), vol. 8, no. 2, February 2011, pp. 309–312.
[26] P. Stoica, A. Nehorai, Performance study of conditional and unconditional direction-of-arrival estimation, IEEE Trans. Acoust. Speech Signal Process. 38 (October (9)) (1990) 1783–1795.